Dual Hardware-In-the-Loop platform for testing and validation of WEC subsystems

Giacomo Alessandri, Federico Gallorini, Joao Cruz, and José Miguel Rodrigues

Abstract—**This paper presents the design process of a dual Hardware-In-the-Loop testing platform targeting components and subsystems of wave energy conversion devices. The platform combines two Hardware-In-the-Loop equipped rigs allowing to simultaneously test components mounted on each rig and connected them to the same simulation environment. A research activity modelling three different device types, three deployment sites and multiple design situations (power production, occurrence of fault, parked) led to a load database which, in combination with information from device developers, defined the requirements for both rigs. The optimal layout, key components and setup of the overall platform were defined according to the specifications and to the results of analyses on mechanical and electrical parameters. The signal processing of each rig was also analysed, with the aim of ensuring dual Hardware-In-the-Loop tests can be performed in a timestep acceptable by the simulation model. An overview of the testing activities that can be conducted within the IMPACT project is presented in this paper, aiming at increasing their maturity through a structured process, with a particular focus on efficiency, reliability and survivability. The proposed approach has the final goal of demonstrating that the platform has the potential of de-risking the technologies from early stages to commercial scale prototype, which is a critical factor for the success of every Wave Energy Converter technology.**

Keywords— **Dual hardware-in-the-loop (DHIL), Wave Energy Converter (WEC); Power Take-Off (PTO); mooring line; dynamic power cable; load analysis; numerical modelling; test methodology; test metrics.**

I. Introduction

THE wave energy sector is currently at an earlier development stage with respect to other renewable energy sources. To date, radically different concepts are stepping slowly through Technology Readiness Levels (TRLs); only few Wave Energy Converters (WECs) have been deployed in real sea conditions, with none of them installed in array configuration [1]. The reasons of the slow progression are multiple and linked either to the harsh deployment environment, characterized by variable and uncertain inputs, either to the high costs required for installing, maintaining, and eventually repairing a damaged subsystem or component. When conceptualizing and developing a device, it is a common practise to design, optimize, verify, and validate the hydrodynamic behaviour of the Wave Energy Converter (WEC) through small-scale tank test, usually adopting scaled proxies of other subsystems such as the Power Take-Off (PTO) and moorings. On one hand, this allows to have a deeper understanding of the concept performances, which are also challenging to represent when scaled down to the tank test model size. On the other hand, the process of selecting and introducing details of real subsystems and underpinning technologies at a later stage require relevant efforts in modelling and laboratory testing activities. A rigorous approach is mandatory to obtain quantitative results, to define the key evaluation areas and associated criteria that can be calculated for each subsystem. These aspects, clearly described and formulated in [2], differentiate the required modelling and testing activities according to the technology development process. Fig. 1 shows that tank testing and dry rig testing acts as parallel process together at almost all the stages. Therefore, it is critical within this second step to undertake all the required activities for validating the characteristics of each subsystem, achieving a more detailed knowledge of the WEC behaviour and a correctly tuned, reliable device model. According to [2], the key evaluation areas that can be targeted in the context of dry rig testing are: power conversion and controllability (herein referred as "performance"), reliability and survivability.

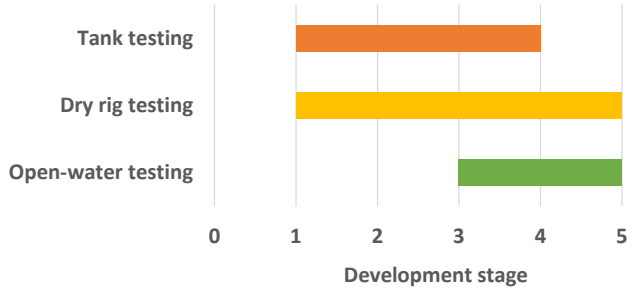

Fig. 1. Type of testing activity at different technology development stages. Derived from [2].

This project has received funding from the European Union's Horizon 2020 research and innovation programme under IMPACT grant agreement No 101007071.

G. Alessandri and F. Gallorini are with VGA S.r.l. the Energy, Via Ugo Foscolo, N.1, 06053 Deruta (PG), Italy (e-mail: giacomo.alessandri@vgasrl.com).

J. Cruz is with Yavin Four Consultants Lda., Rua do Montepio Geral, N.4-B, 1500-465 Lisboa, Portugal (e-mail: joao.cruz@yavinfourconsultants.com).

J. M. Rodrigues is with the Department of Ships and Ocean Structures at SINTEF Ocean, Paul Fjermstads vei 59, Trondheim, Norway (e-mail: Miguel.Rodrigues@sintef.no).

Digital Object Identifier: https://doi.org/10.36688/ewtec-2023-263

TABLE I
TEST PLATFORM INPUT CONSTRAINTS FOR THE DRIVETRAIN TEST RIG

Symbol	Quantity	Unit
*Prated**	100	kW
*Pmax**	250	kW
Stroke	4	m

*Values at actuation system input shaft.

Depending on the development stage the technology is at, each criterium may be calculated for different inputs (e.g. sea states) and boundary conditions (e.g. controllable parameters).

To obtain meaningful results in controlled environments (such as in laboratory) is important to reproduce input conditions which are aligned with the ones the device is subject to in its destination environment; the current state of the art in several sectors (industrial, robotics, automotive, aerospace, power generation) foresees the adoption of simulated environments as a tool to virtually connect the Device Under Test (DUT) to its application. This technique, named as Hardware-In-the-Loop (HIL) or hybrid testing, has been already used also in the wave energy sector as indicated in [3], [4], [5], and [6]. The current work proposes the conceptualization and implementation of a testing approach beyond the state of the art which expands the capabilities of hybrid testing, by implementing it into a novel platform.

II. DUAL HARDWARE-IN-THE-LOOP

WECs are subject to environmental conditions (e.g. wave, tides, wind), mechanical (e.g. mooring or ballast towards the seabed or structures), and electrical (e.g. grid-connected or off-grid systems) constraints, which determine their overall global response (Fig. 1, left). The HIL technique (Fig. 1, centre) consists in the adoption of a simulation platform to virtually replace with a numerical model all the environmental conditions, constraints, and parts of a WEC not subject to the test. Once a certain subsystem has been tested and validated, its behaviour can be described through a numerical model which can be integrated into the global WEC model. This practice aims at refining the ability of the overall device response in different operating and non-operating conditions.

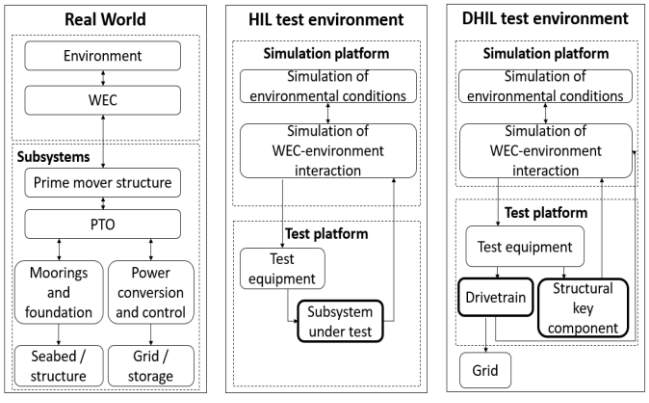

Fig. 2. Real, HIL and dual HIL environments for WECs or its components [7].

Despite the wide recognition of the HIL approach as a state-of-the-art technique which allows to achieve realistic input loading conditions to identify and characterize the DUT key aspects, this technique allows a sole WEC subsystem can be tested at time. When more subsystems are assembled in a device context, interdependencies can be introduced, potentially leading the entire WEC to adopt a different behaviour with respect to the one reproduced by the global simulation model. Interdependencies can only be captured in a numerical model if accurate representations of all the subsystems are accounted for.

The Dual HIL testing scheme combines two HIL equipped rigs that see two different WEC subsystems simultaneously under test (Fig. 1Fig. 2, right). This novel approach allows to test at the subsystems' levels while addressing their influence at a global WEC level (through the numerical model), introducing an increased fidelity. For instance, the energy absorbed by the PTO (through the prime mover) is transferred in parallel to the mooring or foundation system (as a mechanical interface) and to the grid or storage system (as an electrical interface). Being the prime mover, PTO, mooring and power conversion the subsystems usually under stress, a dual HIL test involving a PTO and a mooring system would allow to test and significantly reduce the uncertainties of possible mechanical failures resulting from components interaction under the critical mechanical load path.

Ultimately, the test results can be used to more accurately refine the global WEC model, replicating subsystems inter-dependencies which in turn can inform the future development steps of the WEC design process.

The dual HIL approach is proposed by and implemented within the EU-funded IMPACT project, with the aim of creating a new test platform for WEC developers allowing them to reduce the risk linked to the development of new technologies and the associated costs.

In terms of DUTs, the IMPACT project [7] aims at creating a testing platform addressing the highest number of subsystems that influence the Levelized Cost Of Energy (LCOE) of a device, through the use of two distinctive rigs.

The drivetrain test rig targets linear and rotary PTOs, including control software and hardware, and all required components up to grid interface. Being the drivetrain test rig partially based on a test rig for linear PTOs developed under the EU-funded IMAGINE project [8], the entire work was carried out by considering the related capabilities (shown in Table I), which were set at as boundary design constraints. As a complementary equipment, the structural components test rig allows testing of mechanical components that are part of the prime mover, of the mooring system and dynamic power cables. In alignment with such outline objectives, the analysis and modelling activities conducted within the IMPACT project specifically targeted such critical sub-systems. Being not bound to any existing hardware, no constraints were initially set for the drivetrain test rig, but the simultaneous applicability of the specification derived

TABLE II
WAVE POWER FLUX AT TARGET DEPLOYMENT SITES

Symbol	Quantity	Unit
Pwave at Site#1 – France (3.75W, 48.83N)	17	kW/m
Pwave at Site#2- Spain (7.5W, 43.83N)	21	kW/m
Pwave at Site#3 – Norway (4.5E, 62N)	28	kW/m

from the study of the input condition was addressed at a during the design stage.

In terms of type of test each DUT will be subject to, the key evaluation areas mainly targeted by the IMPACT project are: (1) performance, (2) reliability and (3) survivability. About performance, the recommended test activities in [2] include covering a full range of PTO input conditions, to characterise its functional performance and test the implementation of the control system.

For reliability, [2] specifically refer to test key sub-systems and/or components under cyclic and fatigue loading. Targeting a fatigue strength analysis, possibly with the aim of identifying Fatigue Limit States (FLS), requires an evaluation of cyclic loading that may occur during the lifetime of a WEC.

For survivability, recommended test activities in [2] essentially require examining loading during survival events. This assessment is linked to an ultimate strength analysis, possibly including the investigation into Ultimate Limit States (ULSs). The associated input conditions may be applicable to characterise the required structural strength of PTO, mechanical interfaces, and mooring connections.

III. INPUT SPECIFICATIONS

The definition of the test rig mechanical and electrical input specifications is dependent on the understanding of the load envelope each subsystem or component will be subject to during its lifetime. From a design perspective, such requirements inform the 'demand' profile for the platform. To achieve the proposed test objectives, the 'demand' profile must not exceed the 'supply' profile, i.e. the platform features and overall specifications.

A. Modelling activity

To define the load envelope while targeting the applicability of the test platform to the widest range of device types, a research activity modelling three different WECs, three deployment sites and multiple design situations was conducted. The resulting load database was integrated with information received from WEC developers, to create a more comprehensive specification.

Three device types have been selected, according to a trade-off between modelling feasibility, device type active development status and access to public data: a Submerged Pressure Differential (SPD), a Dual-Body Point Absorber (DBPA) and an Oscillating Wave Surge Converter (OWSC). All these models were conceptualized and implemented in WEC-Sim [10].

The SPD was modelled as a single-body WEC, submerged below the free surface and self-referenced. The meshed geometry was derived from the Reference Model Project [11][12]. The DBPA, a surface located and self-referenced two-body heaving WEC, was generated by scaling down (based on Froude's similitude) the WEC model used in the Reference Model Project [11][12], to align with the constraints indicated in Table I. With the same purpose, also the OWSC, a seabed-mounted and -referenced, surface-piercing oscillating flap, was generated by scaling down the B-OF device of the NumWEC project [13][14]. While SPD and DBPA assumed to integrate a linear PTO, the OWSC is the only device modelled using a rotary PTO. The three geometries are represented in Fig. 3. The wave energy resource characteristics were assessed for a wide number of potential sites (92 data point), with a focus on European waters. The wave resource statistics were derive from long-term hindcast outputs using a third-generation spectral wave model, WaveWatch III (WWIII) [15].

Preliminary WEC performance investigations were also conducted to assess the coupling between environmental conditions and WEC performance from an early stage in the project. A shortlist of wave power flux at the three selected deployment locations is presented in Table II.

While noting that WEC design is outside the scope of work for the IMPACT project, it was assumed that wave

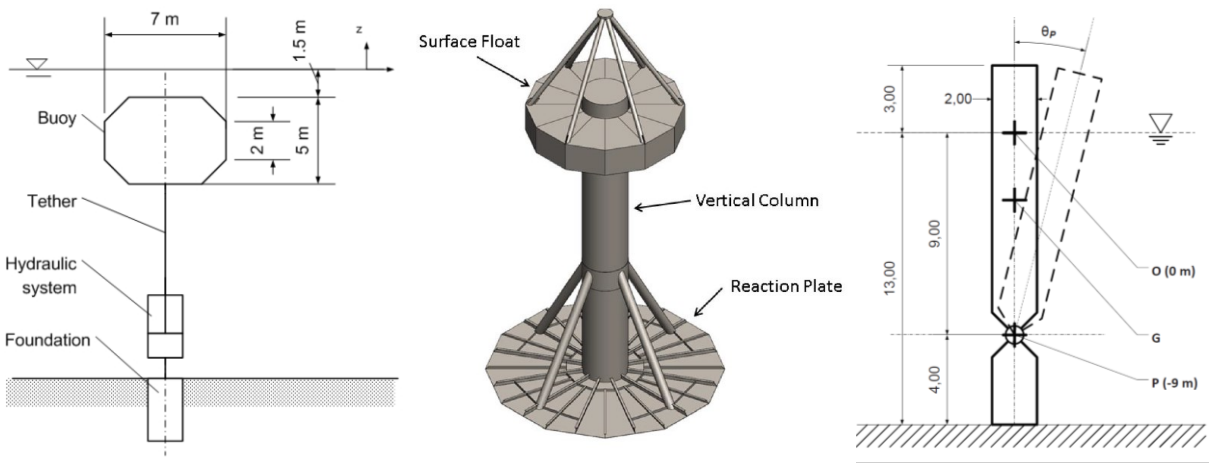

Fig. 3. Baseline WEC models selected for the IMPACT WEC database. [9]

induced loads were dominant in the definition of the load envelope affecting each WEC. Waves were modelled as irregular waves, with a constant direction and no directional spreading. For all the three WECs and for each deployment site, a subset of nine operational cases were in terms of combinations of significant wave height Hs and energy period Te. These, called as as Reduced Normal Sea States (RNSS) range, were used to identify the optimal control parameters for power production. While SPD and OWSC resulted in being optimized with a reactive control (using c_{OPT} and k_{OPT} as control parameters for fixed damping and stiffness, respectively), DBPA optimum configuration resulted in a purely damping control (using only c_{OPT}). The optimal PTO settings are shown in Table III.

Normal Sea States (NSS) were used to assess the loading and kinematic conditions in a design situation of power production, which would inform the specifications associated with normal operation (for performance-related tests) and FLS (for reliability-related tests).

Extreme Sea States (ESS) with 1-year return period were used were used to assess the loading and kinematic conditions in design situations of: (1) power production with the sudden occurrence of a fault (simulated by the loss of damping capability) and (2) parked conditions, with the PTO acting as a brake (fixed constraint). A contour approach was followed for the estimation of the extreme loads: peaks from the specific load time series were by fitted with an extreme value distribution and extracting the 98% quantile of the resulting cumulative density functions (CDFs), leading to an estimate of the 50-year return period load. This procedure was repeated for all the selected sea states on the 1-year contour; the extreme load was then estimated as the maximum of all the calculated 50-year return period loads. These would inform the test platform specifications associated with ULS (for survivability-related tests).

B. Results

The whole set of data was compared to the power constraints set for the rig at the beginning of the project (shown in Table I), to define the final specifications informing the platform design. While the derived PTO mean power estimates, for the three analysed devices (considering operational conditions) is well aligned with the initial target of a 100kW rated PTO rig, the derived PTO peak power estimates often exceed the initial target of a 250kW peak power for the drivetrain test rig.

TABLE III
OPTIMAL PTO SETTINGS FOR POWER PRODUCTION

Symbol	Quantity	Unit
SDP c_{OPT}	75	kN/(m/s)
SDP k_{OPT}	150	kN/(m)
DBPA c_{OPT}	5000	kN/(m/s)
DBPA k_{OPT}	0	kN/(m)
OWSC c_{OPT}	3000	kNm/(rad/s)
OWSC k_{OPT}	1000	kNm/(rad)

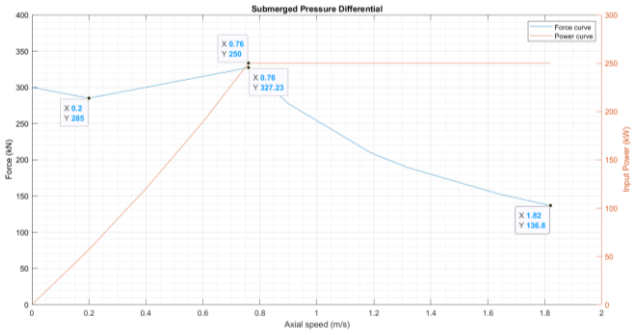

Fig. 4. SPD force and power from power-capped matrix. [9]

As an example, the SPD uncapped matrix was showing a peak force of 360kN for axial speeds up to 2m/s, resulting in a possible peak power of 720kW, far higher that the 250kW constraint. shows the force and power curves related to the SPD where the 250kW constraint was applied. Fig. 4 shows the force and power curves for a curtailment on the maximum power, which is found for a speed of 0.76m/s and for a displacement of 1.8m. At higher speed values, the force may be decreased to ensure compliance with the maximum power limit.

The curves reach a speed value of 1.82m/s, at which the damping-related load would not allow the actuation system to provide an additional displacement the from its equilibrium position since the power has already reached its maximum value. This means that tests where a speed value exceeds the threshold of the first curtailment speed (0.76m/s) should be carefully checked against the displacement expected values before their execution. This approach was also applied to the other WEC models, allowing to define a power envelope required for the motor.

Another aspect to be considered, especially in view of fatigue-related tests, are the damage equivalent loads (DELs): a constant amplitude sinusoidal load that, repeated for N cycles, is estimated to yield the same damage as the original time-varying load. The DEL can be estimated following equation (1):

$$F_{eq} = \left(\frac{1}{N}\sum k\, F_k^m n_k\right)^{\frac{1}{m}} \quad (1)$$

where m is a coefficient that depends on the structural material. In this analysis, it was assumed that the number of cycles N was, for a given sea state, the sea state duration

TABLE IV
DAMAGE EQUIVALENT LOAD (DEL) FOR PTO TESTING

Symbol	QUANTITY	Unit
SDP max DEL from analyses	193	kN
SPD max DEL compatible with control	327	kN
SPD peak speed at which DEL is applicable	1.295	m/s
DBPA max DEL from analyses	1180	kN
DBPA max DEL compatible with control	1118	kN
DBPA peak speed at which DEL is applicable	0.224	m/s
SDP max DEL from analyses	845	kNm
SPD max DEL compatible with control	1595	kNm
SPD peak speed at which DEL is applicable	0.296	rad/s

TABLE V
INPUT SPECIFICATIONS FOR STRUCTURAL COMPONENTS TEST RIG

Symbol	QUANTITY	Unit
SDP DEL	939	kN
DBPA DEL	1180	kN
Mooring A peak force	118	kN
Mooring A stroke	65	mm
Mooring B peak force	1097	kN
Mooring B stroke	251	mm
Power Cable A peak force	813	kN
Power Cable A stroke	210	mm
Power Cable A bending moment	214	Nm
Power Cable B peak force	7.5	kN
Power Cable B stroke	2	mm
Power Cable B bending moment	1053	Nm

divided by the average wave period, and that the material coefficient was m=3 (typical of welded steel).

Table IV summarizes the maximum DEL values related to Site#3, comparing the DEL estimates with the maximum loads resulting from power curves of each modelled device (as the one presented in Fig. 4 for the SPD). It can be noted that all the DELs are within the load envelopes related to the maximum power and the maximum speed at which the load can be applied, to be considered in context of fatigue and accelerated testing.

In addition to the output results from the simulation activity on three numerical models, additional information and data were gathered from WEC developers, to ensure the platform would be able to satisfy the testing needs for different applications in the context of the wave energy sector. Table V presents the peak forces, stroke and bending moment related to mooring lines and power cables testing affecting the structural components test rig, which are found to be included within the maxima resulting from the WEC modelling activity.

Data from WEC developers were also used to compare the PTO power values with respect to the constraints of Table I. While rated values were selected according to WEC developers indications, maximum power values were driven by the three WEC types modelled. These aspects, together with input data for the actuation system selection (e.g. motor torque and speed), are furtherly addressed in the design phase.

C. *Scaling approach*

It is relevant that, for all the three considered evaluation areas (performance, reliability, survivability), [2] suggests that testing for the considered TRLs can be conducted at an appropriate scale, and thus not necessarily at full-scale. In this case, the DUT on the IMPACT rigs would be represented by scaled replicas of the full-scale sub-system under analysis and scaled 'demand' profiles will match the corresponding rig 'supply' power profiles. Under the assumption that inertial and gravitational forces dominate the WEC's dynamics, Froude scaling can be used; this criterium is normally applicable for the main hydrodynamic forces in typical offshore-related problems [16]. For instance, Fig. 5 shows the required scaling factor

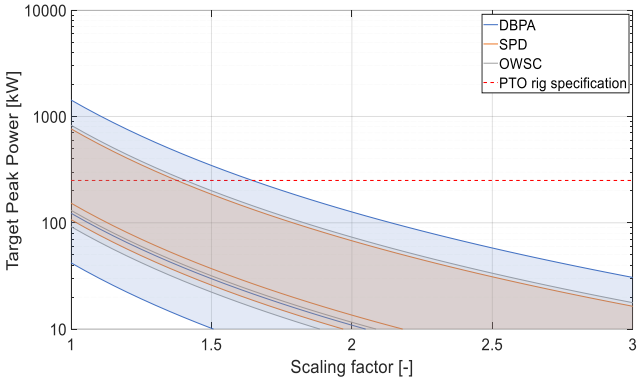

Fig. 5. Peak power scaling chart for the DBPA, SPD and OWSC WEC models. [9]

to match the target peak power of the three WEC types for the operational sea states at target deployment site #3. While the SPD and OWSC devices would require a minimum scale factor of 1.4, the DBPA would require a scale factor of at least 1.6. A similar matching exercise between 'supply' and 'demand' profiles will be executed as a first step for any application involving the usage of the platform, regardless of the key evaluation area of interest.

IV. TESTING PLATFORM DESIGN

The Dual HIL testing platform developed within the IMPACT project has the objective of addressing multiple types of tests on critical subsystems and components within a WEC: characterization tests, for defining key performances of the equipment under test; accelerated tests, to assess qualitative and quantitative reliability features; and ultimate load testing, for survivability purposes. The overall aim of these tests is to identify weaknesses in an early design phase of device design or as a qualification activity prior the deployment of a prototype in real sea environment. To this extent, the design philosophy behind the platform is to ensure the flexibility of each rig towards possible configurations of the DUTs it can target, while allowing complementarity towards subsystems that will be later integrated within a WEC. Finally, each rig should be capable of addressing HIL and accelerated tests, to guarantee these features can be exploited also when the rigs are simultaneously used as a sole testing platform.

A. *Drivetrain test rig*

A set of highly variable input specifications was gathered with the modelling activity of the three WEC types, either in terms of configuration (linear and rotary PTOs), either in terms of range of values. For selecting the components to be integrated into the drivetrain test rig, the input design values have been transformed into standardized parameters that would fit more directly the specification of commercially available components.

To identify a system capable of actuating the PTO input shaft, it was assumed to use mechanical drives (gearbox for rotary PTOs and ballscrews for linear PTOs) coupled to a rotary electrical actuator; the motor operational envelope

TABLE VI
MECHANICAL DRIVE AND GEAR RATIOS FOR THE DRIVETRAIN TEST RIG

Symbol	QUANTITY	Unit
SDP (ballscrew pitch)	160	mm
DBPA (ballscrew pitch)	33	mm
OWSC (gearbox ratio)	240:1	-
WEC A (direct connection)	1:1	-
WEC B (gearbox ratio)	1:5	-
WEC C (ballscrew pitch)	160	mm

can be defined by associating specific torque and speed values to each case study considered. Table VI presents the specific assumptions made for the gear ratio (for rotary PTOs) and pitches (for linear PTOs) to be used. Following the above assumptions, the envelope requested for the rotary actuator was identified, as shown in Fig. 6.

[18] defined indicative conditions to be applied during the drivetrain test rig usage: (1) to consider the possibility to test subsystems singularly (such as the PTO, transmission and control), (2) to have the capability of simulating events of down energy, (3) ensuring the flexibility of the rig in hosting drivetrain with redundant parts and (4) to target failure rates for large-scale components. The aim of these activities is to generate results to be used for addressing techno-economic KPIs, which are relevant in terms of measuring the affordability of a certain WEC technology.

The drivetrain test rig electrical interface towards the DUT should be capable of replicating the test profiles indicated by grid codes and relevant standards [19]. The approach adopted for its selection was to identify a setup able to comply with voltage and frequency values used in different geographical locations across the world. The device to be used as electrical interface should also be able to control a dc bus, allowing to test a PTO in its most basic form, i.e. a generator connected to an ac/dc power converter. Assuming a reference nominal voltage value *Un*, the main capabilities that should be accomplished by a grid emulator were defined in [20] and reported in Table VII. In agreement with the previous recommendations, the drivetrain test rig layout with the DUT having an ac interface is presented in Fig. 7. With the exclusion of the DUT, the rig is divided into three main blocks: mechanical actuation, electrical actuation, and control system.

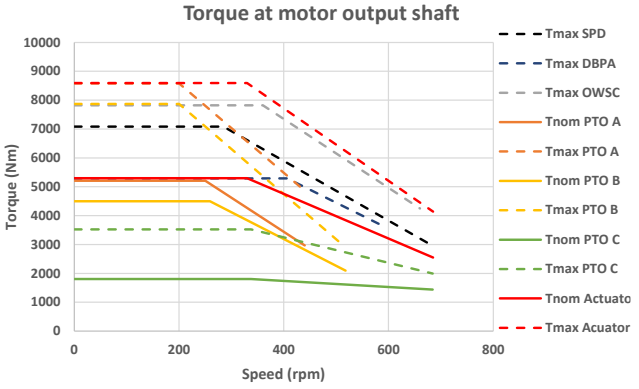

Fig. 6. Rated and maximum speed-torque curves as input specifications for rotary motor of the drivetrain test rig.

TABLE VII
SUMMARY OF DIMENSIONING REQUIREMENTS FOR THE GRID EMULATOR

Symbol	QUANTITY	Unit
Overvoltage capability	1,25**Un*	-
Overvoltage response time	<0.1	s
Undervoltage capability	0.85**Un*	-
Overvoltage response time	0.25	s
Frequency capability for 50Hz grid	47-52	Hz
Frequency capability for 60Hz grid	57-62	Hz
Frequency change	>3	Hz/s
Ramp-up power capability (0-100%)	1	s
Ramp-down power capability (100-0%)	30	s
Shut-down power capability (100-0%)	<2	s

The mechanical actuation system is made up of all the components along the energy conversion chain required to provide a load at the DUT mechanical interface. The new dc/ac converter, motor and torque sensor are added to the transformer and supply unit of the existing rig. The mechanical actuation system is capable of applying the received torque or speed setpoint to the motor output shaft while measuring and sending back these signals in real-time. Other transducers not shown in the figure are the thermal gauges, used to monitor the motor inner and outer temperatures.

The electrical actuation system is in charge of setting a specific profile at the DUT output (electrical) interface. In particular, the grid emulator is capable of receiving a voltage or current setpoint related to a specific grid condition to be tested while sending back the real measured feedback values. A variable input, fixed output transformer can be used in case of ac interface with the DUT. This component would allow to match different output voltages of the DUT with respect to the range 85%-125% *Un* defined in Table VII. The selection of the number and values of voltage levels was carried out by considering to industrial applications in different countries / continents across the world. In case of a DUT having a dc interface, the variable-input, fixed output transformer is bypassed and the dc bus at the motor-side converter output is directly connected to the grid emulator. The setup of the electrical system is designed so that the energy generated by the DUT can be recirculated and used by the mechanical actuation system, with the aim of reducing the oscillation at the grid interface of the facility.

The control system is in charge of sending the setpoints to the mechanical and electrical actuation systems while saving feedback data. In the case of HIL tests, the feedback signals can be elaborated by the real-time simulator to define the setpoint corresponding to the next simulation step. All the components in the mechanical and electrical actuation systems were selected to power and control the motor while covering the entire envelope plotted in Fig. 6. Fig. 7 also shows that in a peak power scenario, considering the efficiency values of commercially available devices and a worst-case scenario of a PTO efficiency of 40%, the power to be absorbed at the grid connection point is at least 295kW. This value was used to size the electrical

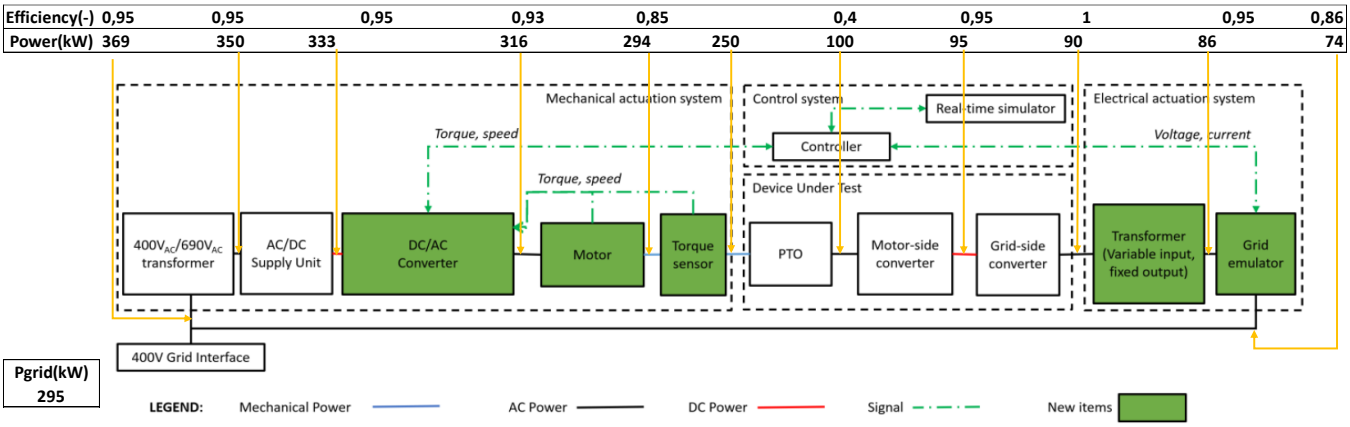

Fig. 7. Drivetrain test rig layout (not all transducers are represented), setup of DUT with an ac interface. On top: peak power levels at each interface and conversion efficiency of each device.

infrastructure the rig is connected to. Fig. 8 shows the mechanical assembly of the drivetrain test rig: on the left side, the rotary motor covering the loading envelope of Fig. 6 is installed, together with a torque sensor. In front of the motor, an empty area can be used to install the DUT and its required interface. On the right side, the same linear actuation system used in the IMAGINE project is adopted. This could be adopted in the case the DUT falls within the loading envelope of the linear actuator, without the need of adding another mechanical drive. The rig structure remains also unchanged, with only the interfaces for the rotary motor and DUT to be added, using the already existing linear rails for their relative positioning.

Table VIII presents the capabilities of the drivetrain test rig at the DUT mechanical and electrical interfaces. Assuming to not exceed the mechanical and electrical power limits presented in Table VIII, the drivetrain test rig design is capable of addressing performance tests, through the definition of typical characterization profiles for mechanical (constant speed for basic testing and HIL for advanced testing) and electrical (normal grid conditions) interfaces by measuring mechanical (through torque transducer and encoder) and electrical data (through the grid emulator) at the interfaces with the DUT. The limited latency allows the execution of real-time simulation models within times compatible with ones currently used in similar applications (3-10ms) [8].

Reliability tests can be executed through the definition of accelerated test profiles, either in position- or load-controlled mode. The rig allows the increase of load, frequency or displacement as acceleration factors. Environmental condition proxies can be applied though the use of focused wave group or regular wave conditions, and DUT degradation can be monitored during time using transducers that can indicate consequence of degradation effects such as the increase of friction and the reduction of efficiency.

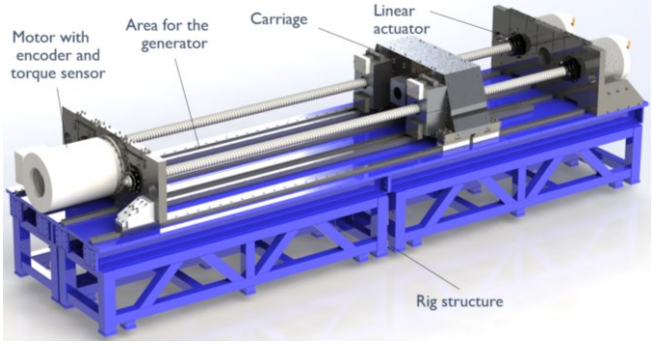

Fig. 8. Drivetrain test rig mechanical assembly render.

Survivability tests can be conducted starting with the characterization of DUT mechanical properties (e.g. stiffness) using load-controlled tests. Once the survivability loading profiles for mechanical (according to a pre-defined value or to a HIL simulation) and electrical (fault or abnormal grid conditions) interfaces are defined, they can be applied through the actuation systems and measurement of structural and electrical loads at the DUT can be conducted during and after the tests (to find out eventual alterations due to permanent damages).

B. *Structural components test rig*

The input specifications summarized in Table V suggest that the structural components test rig should integrate a linear actuator allowing to test full-scale samples of mooring line and power cables, whose loads are aligned with the damage equivalent loads for two different device types (DBPA and SPD). Another actuation system providing at least a rotational degree of freedom to apply bending moments for testing dynamic power cables.

Additional indications from [18] suggested that the rig should allow: (1) to singularly test components such as joints and connections, (2) to test large structural components such as floaters and (3) to ensure the rig is able

TABLE VIII
CAPABILITIES OF THE DRIVETRAIN TEST RIG WITH RESPECT TO DUT MECHANICAL AND ELECTRICAL INTERFACES

Symbol	QUANTITY	Unit
P_{NOM} *mechanical*	220	*kW*
P_{MAX} *mechanical*	300	*kW*
T_{NOM} *mechanical*	480	*kNm*
T_{MAX} *mechanical*	600	*kNm*
ω_{NOM} *mechanical*	330	*rpm*
ω_{MAX} *mechanical*	685	*rpm*
P_{MAX} *electrical*	165	*kVA*
V_{NOM}	495	V_{DC}
V_{MAX}	990	V_{DC}
I_{MAX}	990	A_{DC}

to target failure rates for large-scale components. In terms of testing objectives, the rig should be able to cover the key evaluation areas of reliability and survivability.

Regarding reliability, a specific focus is on testing key sub-systems or components under cyclic and fatigue loading, hence targeting FLSs. This area is primarily covered by the topic of accelerated testing, through the increase of test frequency amplitude, displacement, or environmental stresses.

About survivability, the rig should allow to reproduce loading during survival extreme events, hence targeting ULSs. This key evaluation area should address the maximum value of forces, moments and kinematic conditions required for the rig. Whenever a mismatch between 'supply' and 'demand' profiles is found, the input loads may be scaled following the approach presented in section III, subsection C.

The structural components test rig (Fig. 9) was designed by firstly identifying the possible architecture that could be suitable for the aim of testing mechanical components such as (parts of) the prime mover, mooring system, dynamic power cables and interfaces between subsystems.

Fig. 10 presents the rig layout, characterized by the following details: two different hydraulic actuation systems with single control valves and accumulator mounted nearby are adopted, so that the dynamic response of the system is not subject to delays due to fast changes in the requested flow. The multi-Degree Of Freedom (DOF) actuation system allows to apply a combined bending moment to the DUT, replicating with a higher fidelity the stresses in a case of loading conditions combined with tension or compression. An hydraulic unit is able to supply the required pressure and power flow to the actuators.

The controller is directly interfaced with hydraulic actuation system to send inputs (position, speed, force) and receive outputs (position and load) continuously during tests. The controller is also interfaced with the hydraulic unit to monitor its operation and to identify critical conditions and possible damages on components. On the other side of the DUT, it is assumed that a specific sealing device will be used according to the final layout of the multi-DOF actuation system and to the DUT physical characteristics (e.g. shape, size, stiffness, mass). Four different layouts were evaluated, with the aim of satisfying the layout presented in Fig. 10.

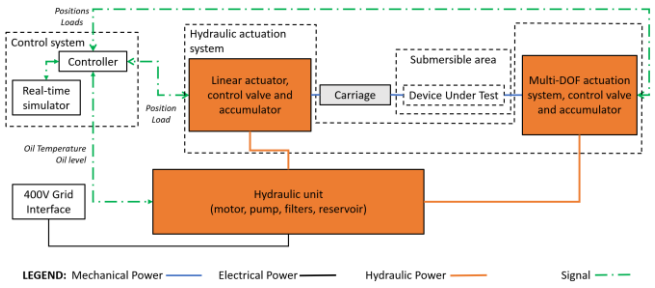

Fig. 10. Structural components test rig layout (not all transducers are represented).

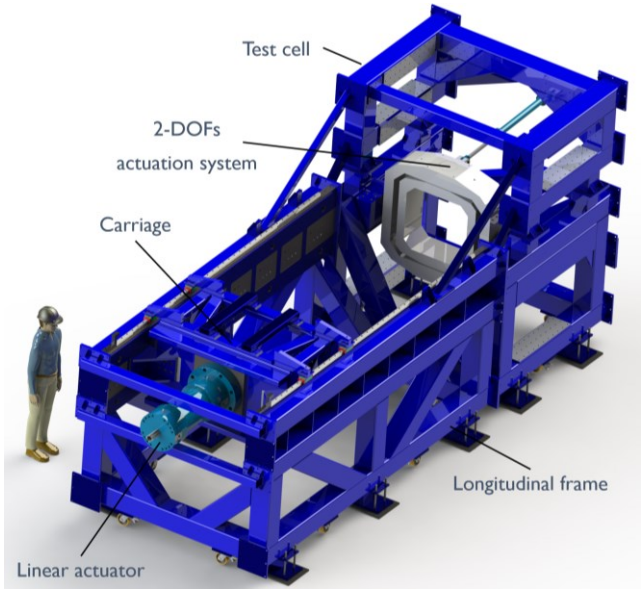

Fig. 9. Structural components mechanical assembly render.

The mechanical assembly of the structural components test rig is shown in Fig. 9. On the left side of the rig, the linear actuator is connected to a tubular frame, capable of being mounted on the rig structure in different longitudinal positions, according to the test sample length. The tubular frame embeds the connection of the linear actuator with the carriage. On the right side, the longitudinal part of the rig is connected to the test cell, a structure made up of two parts (upper and lower), which can host the DUTs. In the figure, the 2-DOFs actuation system is made up of a gimbal joint, connected to the test cell. The inner and outer rings of the gimbal joint are connected to shafts of two linear actuators, mounted on the back of the test cell. In the case of a tests not requiring the presence of the 2-DOFs actuation system, the gimbal and the linear actuators can be disconnected thus increasing the available room within the test cell.

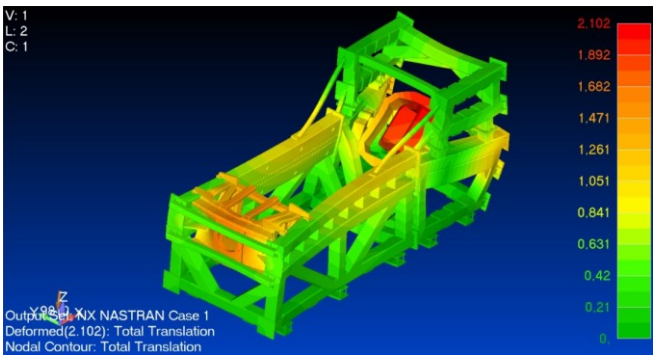

Fig. 11. Deformation of the overall rig structure under compression load on DUT.

TABLE IX
DEFORMATION OF THE RIG STRUCTURE AT DUT INTERFACES

Symbol	QUANTITY	Unit
Deformation at gimbal - compression	1.72	*mm*
Deformation at gimbal - tension	1.76	*mm*
Deformation at linear actuator – compression	1.47	*mm*
Deformation at linear actuator - tension	1.46	*mm*
Total deformation - compression	3.19	*mm*
Total deformation - tension	3.22	*mm*

TABLE X
CAPABILITIES OF THE STRUCTURAL COMPONENTS TEST RIG

Symbol	QUANTITY	Unit
Maximum load – linear actuator	±800	*kN*
Maximum load – 2-DOFs system	±13	*kNm*
Maximum speed – linear actuator	±0.221	*m/s*
Maximum speed – 2-DOFs system	500	*°/s*
Maximum displacement – linear actuator	±0.04	*m*
Maximum displacement – 2-DOFs system	500	°
Maximum sample size – linear actuator	4x1	*m*
Maximum sample size – 2-DOFs system	1.45x1.25x2.5	*m*

The newly designed was verified using Finite Element Analyses (FEAs). Fig. 11 shows the deformation of the overall structure for the compression load case, which resulted being the most critical. The values considered for the analysis of the deformation are the ones in correspondence of the central axis, which are the interfaces with the DUT. These values, summarized in Table IX, should be compared with the deformation expected for the DUT when subject under the same loads. Whenever the values of DUT deformation would be comparable with the deformation of the rig structure, it is recommended to monitor the rig structure through strain gauges, to effectively verify the deformation of the structure is aligned with the result of the model. This value should be discarded from the overall value of deformation measure on the DUT (e.g. by the main linear actuator position transducer). Table X summarizes the capabilities the rig is able to guarantee, considering all the possible mechanical interfaces with the DUT. With respect to the objectives and methodologies presented in section 3 and considering the underlying assumption of not exceeding the mechanical limits presented, the current section demonstrated how the structural components test rig design is capable of measuring mechanical data, through position transducer and load cells at the interfaces with the DUT.

The rig is also able to address reliability tests, through the definition of accelerated test profiles, either in position- or load-controlled mode. The rig allows the increase of load, frequency or displacement as acceleration factors while monitoring of the system degradation during time. For instance, transducers may indicate consequence of degradation effects such as the increase of friction and the reduction of efficiency.

Survivability tests can be addressed through the characterization of DUT mechanical properties (e.g. stiffness), using load-controlled tests. Survivability loading profiles for mechanical interfaces can be defined according to a specified cycle or to a HIL simulation. Measurement of structural deformations of the DUT during the tests and of the performances of the device after the test can be executed, to find out eventual alterations due to permanent damages.

C. *Dual HIL testing platform*

When running dual HIL tests, it is important to consider the number and type of input / outputs that the Real-Time (RT) machine can manage. Fig. 12 shows an example of a test setup where a DUT installed on the structural components test rig and another DUT installed on the drivetrain test rig are using all the available actuation systems (hydraulic system of the structural components test rig, mechanical and electrical actuation systems of the drivetrain test rig). The controllers of the structural components test rig and of the drivetrain test rig mechanical actuation systems are connected through EtherCAT interfaces to the real-time simulator. Dual HIL tests can be run by respectively sending the position and speed signals to the mechanical actuation systems and measuring the force and torque responses. The grid emulator of the drivetrain test rig will contemporarily send a voltage profile through an analog interface and measure the (three-phase) current feedback at the DUT interface. Assuming the numerical model of the WEC is optimally configured to accept the input/output data from the three actuation systems with a latency (related to the execution

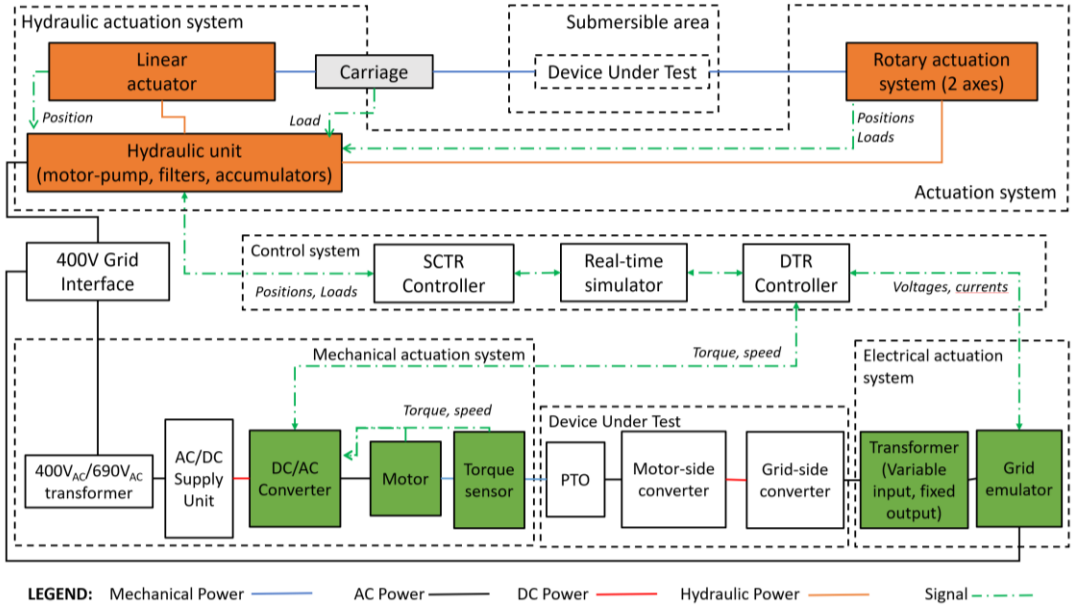

Fig. 12. Example of a dual HIL test setup using the real-time simulator interfaced with both structural components test rigs (SCRT) and drivetrain test rig (DTR) controllers.

of the real-time model) lower than 1ms, the described setup is able to execute the dual HIL test in a range of timestep between 3 and 10ms. This re-configuration could require the adoption of simplified sub-optimal control strategies or modelling techniques, as in [8]. This approach can be adopted within the limits respectively presented in Tables VIII and X and, according to the type of WEC, size and site characteristics can allow to test mid- to full-scale prototypes.

V. Conclusions and Next Steps

This paper presented the dual HIL technique and the methodology with which the testing platform implementing it was designed. Output data from three WEC types and three deployment sites were integrated with inputs from WEC developers, to create a specification envelope for the drivetrain and structural components test rig. Each rig was developed to cater for HIL tests; in addition, the execution of dual HIL tests was ensured by dedicating a specific interface for each actuation system on the RT machine. This feature allows to maintain a suitable timestep for integration with numerical models commonly used in the wave energy sector. The dual HIL platform is therefore a test facility capable of addressing the performance, reliability, and survivability testing of key subsystems (and related components) within a WEC, such as the PTO (electrical machines and mechanical drives), power and conversion system (generator-side and grid-side power converters, control systems, storage systems), mooring system (mooring lines) and power transmission system (dynamic power cables). In addition, mechanical and electrical interfaces could be also tested as part of the DUT. This set of capabilities aims at de-risking the mentioned components before being integrated in a device context. The objective of this approach is to reduce failures associated to open water tests, which are usually capital-intensive activities and therefore representing a high-risk for the successful development of every WEC technology. The future activities within the IMPACT project related to the development of the two rigs and of the testing platform include the commissioning and operation, to demonstrate the key features of the platform using real case studies.

Acknowledgements

The IMPACT project has received funding from the European Union's Horizon 2020 research and innovation programme under grant agreement number 101007071.

References

[1] IEA-OES, "Annual Report: An Overview of Ocean Energy Activities in 2022," Mar 2023. [Online] Available: https://www.ocean-energy-systems.org/documents/54270-oes-report-2022-web.pdf/

[2] J. Hodges., J. Henderson, L. Ruedy, M. Soede, J. Weber, P. Ruiz-Minguela, H. Jeffrey, E. Bannon, M. Holland, R. Maciver, D. Hume, J-L. Villate and T. Ramsey. "An International Evaluation and Guidance Framework for Ocean Energy Technology," 2021. [Online] Available: https://www.ocean-energy-systems.org/documents/47763-evaluation-guidance-ocean-energy-technologies2.pdf/

[3] G. Bacelli, S. Spencer, R. Coe, A. Mazumdar, D. Patterson, K. Dullea, "Design and Bench Testing of a Model-Scale WEC for Advanced PTO Control Research" in Proc. of the *12th European Wave and Tidal Energy Conference*, 2017, Cork, Ireland.

[4] G. Bracco, E. Giorcelli, G. Mattiazzo, V. Orlando M. Raffero, "Hardware-in-the-loop test rig for the ISWEC wave energy system", *Mechatronics*, Vol. 25, pp. 11-17, 2015.

[5] H. Pedersen, R. Hansen, A. Hansen, T. Andersen, and M. Bech, "Design of full scale wave simulator for testing Power Take Off systems for wave energy converters," *International Journal of Marine Energy*, vol. 13, pp. 130–156, Apr. 2016.

[6] S. Armstrong, J. Rea, F.-X. Faÿ, E. Robles, "Lessons learned using electrical research test infrastructures to address the electrical challenges faced by ocean energy developers", *International Marine Energy Journal*, Volume 12, pp. 46-62, 2015.

[7] IMPACT consortium, "Innovative Methods for wave energy Pathways Acceleration through novel Criteria and Test rigs – Technical Annex," April 2020.

[8] G. Alessandri, F. Gallorini, L. Castellini, D. E. Montoya, E. F. Alves and E. Tedeschi, "An innovative Hardware-In-the-Loop rig for linear PTO testing," *International Marine Energy Journal*, *5*(3), 305–314. DOI: https://doi.org/10.36688/imej.5.305-314, [Online].

[9] IMPACT project. D5.1 – Test rigs final specifications report, Issue 01, April 2022.

[10] Y.-H. Yu, K. Ruehl, J. V. Rij, N. Tom, D. Forbush, D. Ogden, A. Keester, and J. Leon, "Wec-sim v4.2," Dec. 2020. [Online]. Available: DOI 10.5281/zenodo.3924764.

[11] V. Neary, M. Previsic, R. Jepsen, M. Lawson, Y.H. Yu, A. Copping, A. Fontaine, K. Hallett, D. Murray, "Methodology for Design and Economic Analysis of Marine Energy Conversion (MEC) Technologies," Sandia National Laboratories, SAND2014-9040. Albuquerque, New Mexico 2014. DOI: 10.13140/RG.2.2.10201.95846, [Online].

[12] K. Ruehl, S.C. Michelén, S. Kanner, M. Lawson, Y.H. Yu, "Preliminary Verification and Validation of WEC-Sim, an Open-Source Wave Energy Converter Design Tool," *Proceedings of the International Conference on Offshore Mechanics and Arctic Engineering – OMAE*, 9, 2014. DOI: V09BT09A040. 10.1115/OMAE2014-24312, [Online].

[13] A. Babarit, J. Hals, M. J. Muliawan, A. Kurniawan, T. Moan, and J. Krokstad, "Numerical benchmarking study of a selection of wave energy converters", *Renew. Energy*, vol. 41, pp. 44–63, 2012. DOI: 10.1016/j.renene.2011.10.002, [Online].

[14] A. Babarit, J. Hals, A. Kurniawan, T. Moan, and J. Krokstad, "The NumWEC project: Numerical estimation of energy delivery from a selection of wave energy converters. Final Report," Ecole Centrale Nantes, Norwegian University of Science and Technology and Statkraft. [Online]. Available: https://www.researchgate.net/publication/275645326_The_NumWEC_project_Numerical_estimation_of_energy_delivery_from_a_selection_of_wave_energy_converters_-_final_report

[15] A. Chawla, D.M. Spindler, and H.L. Tolman, "Validation of a thirty year wave hindcast using the Climate Forecast System Reanalysis Winds," *Ocean Modelling*, Vol. 70, pp 189-206, 2013.

[16] Environmental Conditions and Environmental Loads, DNV-RP-C205, 2014.

[17] IMPACT project. D6.1 – Drivetrain test rig design report, Issue 01, December 2022.

[18] IMPACT project. D4.1 – Techno-economic specifications report, Issue 01, January 2022.

[19] *Marine energy - Wave, tidal and other water current converters - Part 30: Electrical power quality requirements*, IEC TS 62600-30:2018, 29/08/2018.

[20] IMPACT project. D3.1 – Review of grid codes, Issue 01, October 2021.